

Scheme for generation of flat top and high signal-to-noise ratio optical frequency comb

Jianrui Li (李建蕊), Jiachuan Lin (林嘉川), Xiaoguang Zhang (张晓光)*, Lixia Xi (席丽霞), Xianfeng Tang (唐先锋), and Yaojun Qiao (乔耀军)

State Key Laboratory of Information Photonics and Optical Communications, Beijing University of Posts and Telecommunications, Beijing 100876, China

*Corresponding author: xgzhang@bupt.edu.cn

Received August 12, 2014; accepted November 14, 2014; posted online January 5, 2015

We demonstrate a new scheme for generation of optical frequency comb (OFC) based on cascade modulators, 23 comb lines within 0.5 dB spectral power variation are obtained. An optical finite impulse response (FIR) filter is introduced for suppression of amplified spontaneous emission noise. It is shown that carrier-to-noise-ratio of the OFC generated by this scheme can be as high as 38.8 dB with 12 dB improvement by using a 16-tap FIR filter, and the error vector magnitude performances of loaded Nyquist-16 quadrature amplitude modulation signal is improved from 14.20% to 7.44%.

OCIS codes: 060.0060, 060.5060, 350.2460.

doi: 10.3788/COL201513.010605.

Optical frequency comb (OFC), which is also called multi-carrier, is a series of equally spaced spectral comb lines^[1]. With the development of technique, its application has been extended to many aspects, such as ultra-short pulse generation^[2], arbitrary waveform generation^[3], and dense wavelength division multiplexing^[4]. In particular, the combination usage of OFC technology and high-order modulation pattern as a solution of terabit transmission has become the development direction of next-generation fiber-optic communication^[5,6]. Many endeavors have been made on generation of OFC including exploiting fiber loop modulation^[7], mode-locked lasers^[8], re-circulating frequency shifter^[9-11] and cascaded modulators^[12-14]. Among these technologies, cascaded modulators to generate OFC have attracted intensive attention due to its phase-correlated, frequency spacing tunability and large bandwidth with a relatively low-amplitude radio frequency (RF) driving signal. This kind of scheme is based on the principle that includes two key procedures to obtain a high-quality OFC^[12]. At first, a series of flat-topped pulses are generated in time domain, and then are converted from time-to-frequency domain which is equivalent to mapping the intensity shape of a single pulse into the frequency domain. The function of the former can be implemented by an intensity modulation, whereas the function of the latter can be implemented by a parabolic phase modulation. Non-flat spectral envelope of the comb may limit some of its applications^[15,16]. Several efficient solutions have been proposed and demonstrated to improve the degree of flatness. Wu *et al.*^[17] reported 38 comb lines within 1 dB spectral power variation. They used cascaded intensity modulator (IM) and phase modulator (PM). The IM generated the flat-topped pulses which realized the first procedure of the abovementioned principle, and the PM was driven by specially tailored RF waveform which induced an approximation to parabolic temporal phase

in the second procedure. Apparently, the complicated RF devices might be needed in the second procedure, which makes the scheme difficult to be implemented. Dou *et al.*^[18] reported another improvement of flatness of OFC based on nonlinear effect of IM, whose simulation results display that with the resolution of optical spectral analyzer 1.25 GHz, the spectral power variation is about 1 dB, but with higher resolution such as 24.3 MHz, the spectral power variation expands to about 4 dB, which is not flat enough for application. Therefore, the generation of a sufficient flat optical comb is still a challenging task which is worth trying for further improvement. At the same time, the scheme in Ref. [18] generates a dozen or even dozens of comb lines at one time which leads to the input power allocated to many subcarriers, the signal-to-noise ratio (SNR) of each carrier is not high enough for its application, such as loading higher order modulation signal. Liu *et al.*^[5,6] proposed using erbium-doped fiber amplifier (EDFA) to amplify the optical comb before loading the signal to extend transmission distance; however, the amplified spontaneous emission (ASE) noise will also be amplified which will result in a deterioration of the SNR of optical comb.

In this letter, we propose a new modified scheme for optical comb generation based on cascade modulators with higher flatness which relies on a trade-off of the good features that the abovementioned two procedures would seek. Furthermore, an improved configuration with ASE noise suppression scheme using optical finite impulse response (FIR) filter is demonstrated^[19]. By applying this scheme, an obvious carrier-to-noise-ratio (CNR) performance improvement is achieved.

As mentioned above, in order to get a large number of flat and high-quality OFC, the conventional scheme using cascaded modulators is based on the principle that includes the two key procedures. At first, flat-top

pulse train by intensity modulating a continuous wave laser is prepared, and then are modulated with a parabolic temporal phase by $\exp(iKt^2/2)$, where K is the chirping rate. The higher the degree of flatness of the pulse train in time domain, the more flat the OFC in frequency domain, through a time-to-frequency conversion which is implemented by phase modulation of $\exp(iKt^2/2)$. The scaling of the envelope of comb or the effective number of comb lines is determined by $n \propto \frac{|K|}{\omega_m}$, where $\omega_m = \frac{2\pi}{T}$ and T is the period of the pulse train. The intensity modulation can be implemented by Mach-Zehnder IM (MZIM) whose transfer function is

$$T_I = \cos \left[\frac{\pi}{2V_\pi} (V_I \cos(\omega_m t) + V_{\text{IDC}}) \right], \quad (1)$$

where V_I is the amplitude of cosine RF signal applied on MZIM, ω_m is the microwave angular frequency, V_π is the half-wave voltage, and V_{IDC} is the bias voltage. The generated flat-topped pulse train by a MZIM with $V_I = 0.5V_\pi$ and $V_{\text{IDC}} = 0.5V_\pi$ is shown in Fig. 1(a). The phase modulation can be implemented by PM whose transfer function is

$$T_p = \exp(i\Phi(t)), \quad (2)$$

where $\Phi(t)$ is the temporal phase function. Ideally, it should be exactly a parabolic shape $\Phi(t) = Kt^2/2$. As shown in Fig. 1(a), the coefficient K takes the value -0.758×10^{23} . The comb lines in frequency domain generated by the conventional scheme of cascade of MZIM and PM are shown in Fig. 1(b).

Unfortunately, in practice, it is not easy to produce a parabolic function applied on the PM. Instead, the cosine function is easily implemented to substitute the difficult parabolic modulation

$$T'_p = \exp \left[i \frac{\pi}{V_\pi} \cdot V_p \cos(\omega_m t) \right], \quad (3)$$

where V_p is the amplitude of cosine microwave signal. However, as the resultant effect, the generated OFC using a cosine signal (Fig. 1(c)) instead of the ideal parabolic applied on the PM is generally not flat enough as shown in Fig. 1(d) with $V_p = 17$ V, and the peak power variance of 23 comb lines is 5.5 dB with 24.3 MHz resolution. The corresponding flat-topped pulse and cosine phase function are shown in Fig. 1(c). Taking a step back, if the parabolic function can be realized, and we load $V_I = 0.5V_\pi$, $V_{\text{IDC}} = 0.35V_\pi$ on IM, the pulse in time domain is less flat and the pulse width is narrower than that in Fig. 1(a) as shown in Fig. 1(e). The corresponding comb lines generated in frequency domain by this scheme are also inferior to Fig. 1(b) as shown in Fig. 1(f). In conclusion, these two kinds of combination of the pulse train generation and phase modulation do not produce

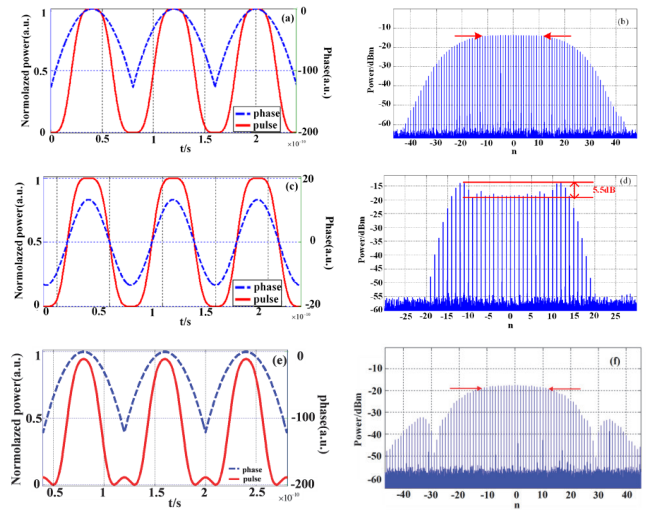


Fig. 1. Simulation results of pulse train profile and the phase function on the left side with the corresponding OFC on the right side.

good results. But the miracle will occur if we use the trade-off strategy as describe below.

In order to improve the comb flatness in practical application, we propose that we can make a trade-off between the abovementioned two key procedures, which is the effort to obtain more flat-top pulse train and the aspiration to get a parabolic-shaped phase modulation. Dou *et al.*^[18] reported that using the combination of $V_I = 0.5V_\pi$ and $V_{\text{IDC}} = 0.35V_\pi$ loaded on IM to compress pulse width and cosine function with $V_p = 17$ V loaded on PM which is the cross-over combination of Figs. 1(c) and (e) as shown in Fig. 2(a), the corresponding comb line generated in Fig. 2(b) has 1 dB variation in 1.25 GHz or 4.2 dB in 24.3 MHz resolution which is more flat than Fig. 1(d). But the flatness is still not enough for the applications such as pulse sharpening and

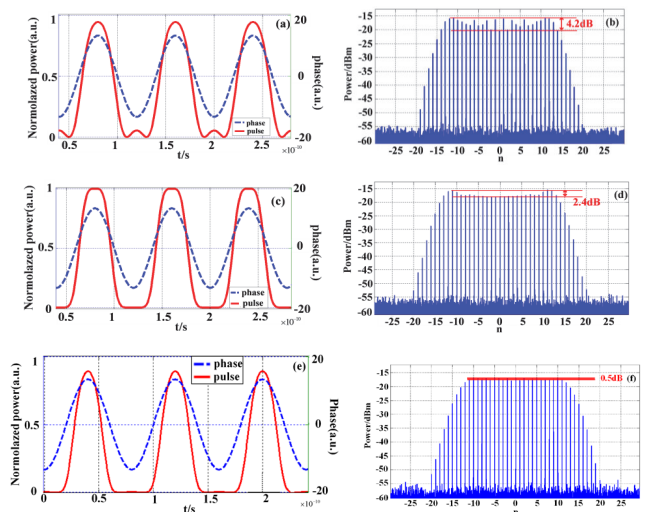


Fig. 2. Simulation results of OFC on the right side with the corresponding pulse train profile and the phase function on the left side using the trade-off strategy.

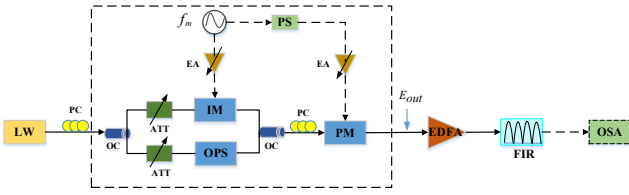


Fig. 3. Proposed optical comb generation scheme.

high-order modulation such as m -quadrature amplitude modulation (QAM).

Based on the above trade-off theory, a new scheme of combination of MZIM and PM to generate more flat comb lines is shown in dashed frame in Fig. 3, which consists of two 50:50 couplers, two electrical power amplifiers, an IM, an electrical phase shifter (PS), an optical PS (OPS), and a PM. The electrical PS here is used to adjust the RF phase difference between IM and PM. What needs to be noted is that an OPS is added on the lower arm paralleling with IM in comparison with the traditional scheme, two adjustable attenuators are used to adjust balance of the optical powers in two arms. The function of the OPS here is used to adjust phase difference between the two arms. Assuming that the phase change introduced by IM on the upper arm is zero, then the phase shift by the OPS will be set as zero. The total transfer function of the proposed scheme can be changed as

$$\begin{aligned} T_{\text{total}} &= (T_I + 1)T_P' = T_I' T_P' \\ &= \left[\cos \left[\frac{\pi}{2V_\pi} (V_I \cos(\omega_m t) + V_{\text{IDC}}) \right] + 1 \right] T_P' \\ &= 2 \cos^2 \left[\frac{\pi}{4V_\pi} (V_I \cos(\omega_m t) + V_{\text{IDC}}) \right] T_P', \quad (4) \end{aligned}$$

where T_I in Eq. (1) is replaced by T_I' because we use the parallel structure of MZIM and OPS instead of only MZIM. Based on the abovementioned two procedures principles, for the reason that we use the easily implemented cosine shape phase modulation instead of the parabolic shape in the second procedure, we make a trade-off strategy that slightly reduces the range of flat top of the pulse shape in the first procedure. We all know that the width of the pulse train function T_I' whose shape is a cosine-squared function is narrower and less flat than T_I whose shape is a cosine function. So with the new scheme, the flatness of pulse train is slightly reduced. And then in the narrow range of the flat top of the pulse the phase function with the cosine shape is more approximate to the parabolic, or in other words, the less flat-top pulse shaping can weaken or compensate the negative effect of non-ideal parabolic phase modulation, and as a result, leading to a more flat comb lines. The pulse train generated by T_I' with $V_I = V_\pi$ and $V_{\text{IDC}} = V_\pi$ is shown in Fig. 2(c), which is less flat and narrower than T_I shown in Fig. 1(c). The corresponding comb lines after phase modulated by

$\Phi(t) \propto \cos(\omega_m t)$ with $V_p = 17$ V are shown in Fig. 2(d) with 2.4 dB peak power variation with 24.3 MHz resolution. It is obvious that the comb lines flatness has a better performance than that of Fig. 1(d) or even better than that of Fig. 2(b), which shows the validity of our scheme.

Furthermore, we try a bias point at $V_{\text{IDC}} = 0.7V_\pi$ instead of $V_{\text{IDC}} = V_\pi$ which utilizes the nonlinearity of modulation curve of the MZIM to further slightly reduce the flatness of the pulse train. Then the phase function will be more approximate to the parabolic than that with $V_{\text{IDC}} = V_\pi$. The corresponding comb lines after phase modulated by cosine function with $V_p = 17$ V are shown in Fig. 2(f), and the corresponding pulse train and the phase function are shown in Fig. 2(e). Then 23 comb lines within 0.5 dB spectral power variation with the resolution of optical spectrum analyzer 24.3 MHz are generated, which is the best result of the schemes based on cascaded IM and PM to the best of our knowledge.

In order to apply the generated comb lines into optical fiber super-channel communication system, and load the multi-level modulation formats on them, the SNR of the optical comb lines should be improved. Generally, we must use an EDFA to amplify the comb lines, with the result that the ASE noise will be introduced. Therefore, the suppression of ASE noise must be implemented. We propose a noise suppression scheme of FIR filter which is discussed in detail as follows.

For N -tap FIR filter, if the tap coefficient of each arm is $1/N$ (case 1), which can constitute the parallel structure as shown in Fig. 4(a), the amplitude transfer function can be expressed as

$$\begin{aligned} F_{\text{FIR}}(\omega) &= \frac{1}{N} \cdot [1 + \exp(-j\omega\tau) + \exp(-j2\omega\tau) \\ &\quad + \exp(-j3\omega\tau) + \dots + \exp(-j(N-1)\omega\tau)]. \quad (5) \end{aligned}$$

Then the power transfer function is

$$\begin{aligned} P_{\text{FIR}}(\omega) &= F_{\text{FIR}}(\omega) \cdot F_{\text{FIR}}^*(\omega) \\ &= \frac{1}{N^2} \{ N + 2[(N-1)\cos\omega\tau + (N-2)\cos 2\omega\tau + \dots \\ &\quad + \cos(N-1)\omega\tau] \} \\ &= \frac{1}{N} + \frac{2}{N^2} \cdot \sum_{n=1}^{N-1} (N-n) \cdot \cos(n\omega\tau), \quad (6) \end{aligned}$$

where τ is the time-delay unit. A free spectrum range equal to channel spacing f_m is expected here so that τ

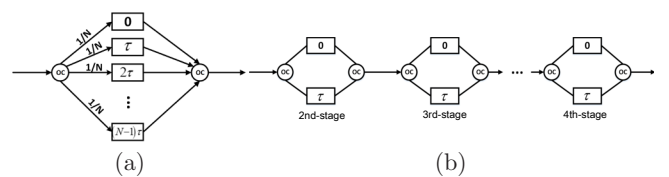


Fig. 4. (a) Implementation of optical FIR filter for ASE noise suppression described in case 1 and (b) implementation of optical FIR filter for ASE noise suppression described in case 2.

has a value of $1/f_m$. The performances of the FIR filters with tap numbers 2, 4, and 8 are shown in Fig. 5(a). The ASE noise power passing through the N -tap optical FIR filter can be expressed as

$$P_{\text{out, ASE}} = \int_{\omega-2\pi f_m/2}^{\omega+2\pi f_m/2} S_{\text{in, ASE}}(\omega) P_{\text{FIR}}(\omega) d\omega, \quad (7)$$

where $S_{\text{in, ASE}}$ is the power spectral density of the ASE noise. We find that

$$P_{\text{out, ASE}} = \frac{1}{N} \cdot P_{\text{in, ASE}}. \quad (8)$$

In the system the power and the wavelength of the optical source are 11.5 dBm and 1559.59 nm, the frequency of the RF signal is 10.7 GHz. In addition, the saturated output power of EDFA is set as 24.5 dBm, the insertion losses of IM, PM, and filter are about 3, 3, and 1.5 dB, respectively, and the resolution of optical spectrum analyzer is 24.3 MHz. The simulation results of the optical comb passed through the 8-tap FIR filter is shown in Fig. 6, which gets an evidently ASE noise suppression compared with that in Fig. 2(f). Theoretical and simulation results prove that after the FIR filter the performance of comb lines is improved significantly.

For N -tap FIR filter, if the tap coefficient of m th arm is $\left(\frac{1}{2}\right)^m \cdot C_N^m$ (case 2), which can constitute the N -stage serial structure as shown in Fig. 4(b), the amplitude transfer function can be expressed as

$$F_{\text{FIR}}(\omega) = \left(\frac{1}{2}\right)^N \left[1 + \exp(-j\omega\tau)\right]^N. \quad (9)$$

Then the power transfer function is

$$\begin{aligned} P_{\text{FIR}}(\omega) &= F_{\text{FIR}}(\omega) \cdot F_{\text{FIR}}^*(\omega) \\ &= \left(\frac{1}{2}\right)^{2N} \left(C_N^0 1^N \cos(\omega\tau)^0 + C_N^1 1^{N-1} \cos(\omega\tau)^1 \right. \\ &\quad \left. + \dots + C_N^{N-1} 1^1 \cos(\omega\tau)^{N-1} + C_N^N 1^0 \cos(\omega\tau)^N \right) \\ &= \sum_{m=0}^N C_N^m \cdot \left(\frac{1}{2}\right)^{2N} \cdot \cos^m(\omega\tau), \end{aligned} \quad (10)$$

τ also has a value of $1/f_m$. The performances of the FIR filters with stage numbers 2, 4, and 8 are shown in

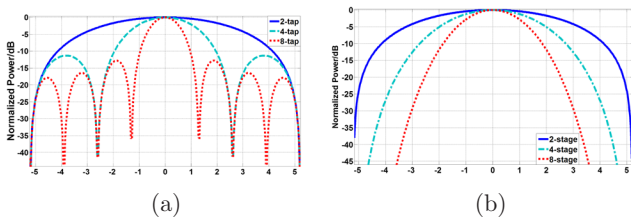


Fig. 5. (a) Power transfer function of optical FIR filter with different tap coefficients described in case 1 and (b) power transfer function of optical FIR filter with different stage coefficients described in case 2.

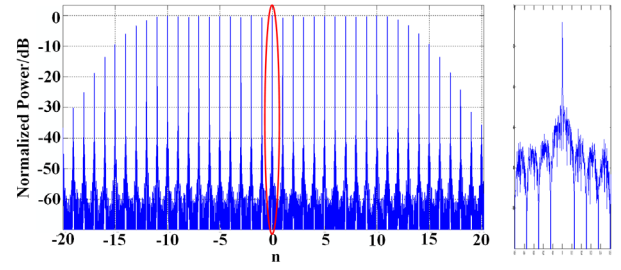


Fig. 6. 23 comb lines generation passed through 8-tap FIR filter and zoom version of middle comb.

Fig. 5(b). The ASE noise power passing through N -stage optical FIR filter can be expressed as

$$P_{\text{out, ASE}} = \frac{1 + \sum_{m=1}^{\lfloor N/2 \rfloor} C_N^{2m} \cdot \frac{(2m-1) \cdot (2m-3) \cdot \dots \cdot 3 \cdot 1}{2m \cdot (2m-2) \cdot \dots \cdot 4 \cdot 2}}{2^N} \cdot P_{\text{in, ASE}}. \quad (11)$$

The simulation results about the optical comb passed through the 8-stage FIR filter is shown in Fig. 7, which also bring an evident ASE noise suppression compared with that in Fig. 2(f). The ASE noise suppression of the serial scheme is not as good as the parallel one, but is also effective and maybe easier to implement.

In order to evaluate the performance of the high-quality optical comb lines generated with the scheme proposed in this work, when they are applied to a super-channel optical fiber communication system, we make a simulation system as illustrated in Fig. 8. In this simulation system, the comb lines are separated by the demultiplexer and then sent into the IQ modulator. The 4-level driven signals with square-shaped spectrum applied on I and Q branches are generated with 128 order digital raised cosine FIR filter with rolloff = 0. Each carrier is loaded with 28 Gbaud Nyquist-16 QAM signal. Then the interesting comb line loaded on signal is selected with a 10-order super-Gaussian filter with bandwidth of f_s and detected with coherent detection. In order to evaluate the influence of the ASE noise on the light source more exactly, both the linewidths of signal source and local oscillation are set to 0 kHz, and digital signal processing part without using a phase compensation algorithm.

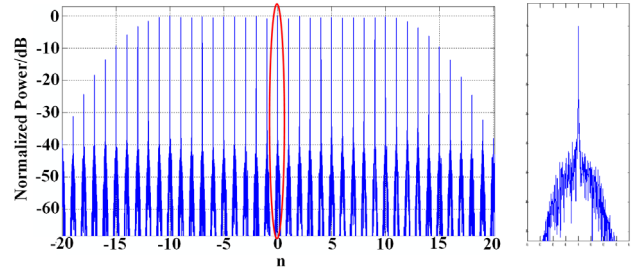


Fig. 7. 23 comb lines generation passed through 8-stage FIR filter and zoom version of middle comb.

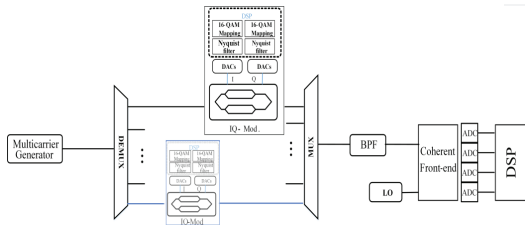


Fig. 8. Transmission system with Nyquist-16 QAM loaded on the comb lines.

In this work, we define $CNR^{[19]}$ to accurately evaluate the ASE noise of each comb line instead of tone-to-noise ratio (TNR) in other works^[20]. TNR may be a suitable indicator to measure the performance of optical comb with flat noise floor, but for non-flat noise floor shown in Figs. 6 and 7 CNR is a better choice. CNR of n th carrier with (12.5 GHz) 0.1 nm reference noise bandwidth which is similar to optical SNR is defined as

$$CNR_n = 10 \lg \left(\frac{P_{\text{carrier}}}{P_{\text{ASE}, n}} \right). \quad (12)$$

The calculation results of CNR of the comb passing through the different tap numbers or stage numbers of parallel and serial FIRs are shown in Fig. 9. With 28 Gbaud Nyquist-16 QAM loaded on the comb, the constellations of signals are also shown in Fig. 9. As is depicted in Fig. 9, the blurred constellation loaded on the comb with no FIR filter is observed, which has an error vector magnitude (EVM) of 14.20%. Clear QAM patterns with 8-tap or 16-tap FIR filter are obtained surprisingly, which have the EVMs of 9.11% and 7.44%, respectively. It suggests that our schemes can effectively improve the quality of the comb source.

As revealed above, the evaluation using CNR for the naked carrier tone is closely related to the evaluation using EVM for the quality of loaded signal, which also implies the performance of whole transmission system. The EVM performances of the loaded Nyquist-16 QAM signal when applying proposed ASE noise suppression scheme with different taps or stage numbers is shown in Fig. 10. It is obvious that the optical comb without FIR filter cannot support

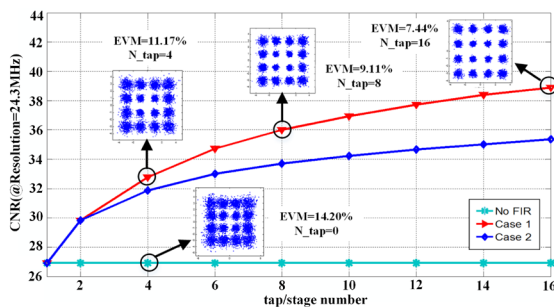


Fig. 9. CNR of the selected comb with optical FIR filter and constellations of loaded signal on the comb.

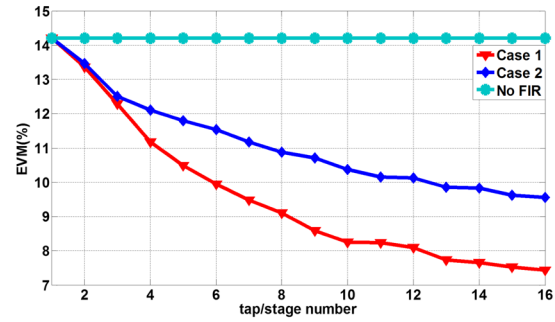


Fig. 10. EVM performances of loaded Nyquist-16 QAM signal when applying proposed ASE noise suppression scheme with different tap or stage numbers.

high-order modulation format system, whereas a distinct improvement can be found when using the proposed optical FIR filter-based ASE noise suppression scheme, which can help improve the EVM from 14.20% to 7.44% or even better. We can see that the high-quality optical comb generated by the proposed scheme is very suitable for super-channel optical fiber communication system (such as Nyquist, WDM, or OFDM) with the higher order modulation formats (such as 16 QAM or 32 QAM).

In conclusion, we demonstrate a new scheme for optical comb generation based on cascade modulators, the generated comb lines can be obtained within 0.5 dB spectral power variation. Compared with the previous scheme, it really has better flatness and is also easy to implement. To improve CNR performance of the optical comb, a noise suppression scheme based on FIR-filter is proposed and theoretically analyzed. The simulation results indicate that CNR can achieve the improvement of about 8.4 dB (16-stage) and 12 dB (16-tap), which is consistent with theoretical results. Furthermore, a 28 Gbaud Nyquist-16 QAM format is loaded on the comb lines, a distinct improvement can be found, that is, the EVM of the constellation of the signals loaded on the comb is improved from 14.20% to 7.44% or even better, which is suitable for super-channel optical fiber communication systems.

This work was supported by the National Natural Science Foundation of China (No. 61205065), the National 863 Program of China (No. 2013AA013401), and the Open Fund of IPOC (BUPT; No. IPOC2013B005).

References

1. J. Ye and S. Cundiff, *Femtosecond Optical Frequency Comb: Principle, Operation and Applications* (Kluwer Academic Publishers/Springer Norwell, 2004).
2. Z. Jiang, C. B. Huang, D. E. Leaird, and A. M. Weiner, *Nat. Photon.* **1**, 463 (2007).
3. S. T. Cundiff and A. M. Weiner, *Nat. Photon.* **4**, 760 (2010).
4. F. Tian, X. Zhang, L. Xi, A. Stark, S. E. Ralph, and G. K. Chang, *Opt. Eng.* **52**, 116103 (2013).
5. X. Liu, S. Chandrasekhar, X. Chen, P. Winzer, Y. Pan, B. Zhu, T. Taunay, M. Fishteyn, M. Yan, M. Fini, J. E. Monberg, and F. Dimarcello, *Opt. Express* **19**, B958 (2011).

6. J. Yu, Z. Dong, J. Zhang, X. Xiao, H. C. Chien, and N. Chi, *J. Lightw. Technol.* **30**, 458 (2012).
7. M. Hirano and A. Morimoto, *Opt. Rev.* **18**, 13 (2011).
8. F. Quinlan, S. Ozharar, S. Gee, and P. J. Delfyett, *J. Opt. A: Pure Appl. Opt.* **11**, 103001 (2009).
9. T. Kawanishi, T. Sakamoto, S. Shinada, and M. Izutsu, *IEICE Electron. Express* **1**, 217 (2004).
10. J. Li, X. Zhang, F. Tian, and L. Xi, *Opt. Express* **19**, 848 (2011).
11. H. Zhou, L. Xi, J. Li, X. Zhang, and N. Liu, *Chin. Opt. Lett.* **10**, 100602 (2012).
12. J. Lancis and P. Andrés, *Opt. Lett.* **33**, 1822 (2008).
13. Y. Yu, Z. Dong, and N. Chi, *IEEE Photon. Technol. Lett.* **23**, 1061 (2011).
14. S. Zou, Y. Wang, Y. Shao, J. Zhang, J. Yu, and N. Chi, *Chin. Opt. Lett.* **10**, 070605 (2012).
15. M. Fujiwara, M. Teshima, J. I. Kani, H. Suzuki, N. Takachio, and K. Iwatsuki, *J. Lightw. Technol.* **21**, 2705 (2003).
16. Y. Yamamoto, T. Komukai, K. Suzuki, and A. Takada, *J. Lightw. Technol.* **27**, 4297 (2009).
17. R. Wu, V. R. Supradeepa, C. M. Long, D. E. Leaird, and A. M. Weiner, *Opt. Lett.* **35**, 3234 (2010).
18. Y. Dou, H. Zhang, and M. Yao, *Opt. Lett.* **36**, 2749 (2011).
19. J. Lin, L. Xi, J. Li, X. Zhang, X. Zhang, and S. A. Niazzi, *Opt. Express* **22**, 7852 (2014).
20. J. Zhang, J. Yu, N. Chi, Z. Dong, Y. Shao, L. Tao, and X. Li, *IEEE Photon. J.* **4**, 2249 (2012).